

# Microstructural Evolution in IN718 Produced by L-PBF Additive Manufacturing

Hyeyun Song, Project Engineer  
EWI

## Introduction

Laser powder bed fusion (L-PBF) is an additive manufacturing (AM) process, enabled by computer-aided design (CAD)<sup>1,2,3</sup>, in which a laser beam is applied to melt fine metallic powders, then deposited layer by layer. Using L-PBF for manufacturing complex, shaped parts can save both time and cost due to improved process precision and reduced post-build processing. L-PBF (also known as “selective laser melting”) is being increasingly applied to produce various metal components using a wide range of materials and alloys.

## Nickel base super alloy, Inconel® 718

Inconel® 718 (IN718), a nickel-based superalloy, is a workhorse alloy for L-PBF due to its superior performance at high temperatures. IN718 can withstand heating up to 700°C including stain-age cracking<sup>4</sup>. IN718 is strengthened by both  $\gamma''$  (Ni<sub>3</sub>Nb) and  $\gamma'$  (Ni<sub>3</sub>(Ti,Al)) precipitates, which are normally formed during post heat treatment. Knorovsky et al. observed the formation of other precipitates in IN718, including Laves phase (Ni<sub>2</sub>Nb), Nb-rich carbide (NbC), and delta phase (Ni<sub>3</sub>Nb). These second phase precipitates are typically generated during solidification<sup>5</sup>. Due to its brittle characteristics, it is necessary to minimize the formation of the Laves phase during both solidification and post-heat treatment. As discussed by Manikandan et al.<sup>6</sup>, Nb, an alloy element of IN718, is consumed during the formation of the Laves phase resulting in the reduction of the fraction of the strengthening precipitates  $\gamma''$  and  $\gamma'$ .

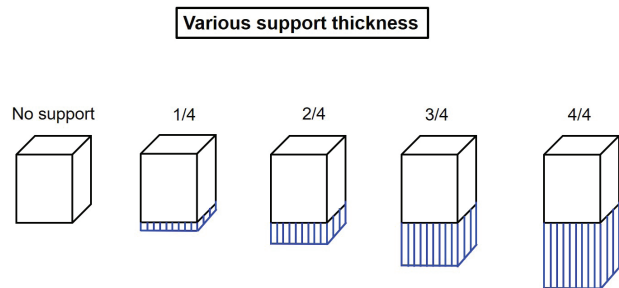
## Effect of Support

For complex geometries, such as overhanging parts, sacrificial structures are utilized to support the primary geometry<sup>4</sup>. These supportive structures are subsequently removed after the build is complete. The support structures prevent or reduce thermal expansion resulting from the non-uniform and repeated spatial heating and cooling during the deposition. Optimization of the support design, investigated by Krol et al.<sup>7</sup>,

showed that reduction of the support areas enhanced the support stiffness. The support structure has smaller cross-sectional area compared to the primary structure, but larger cross-sectional area compared to the metal powders existing in the layer. Even though the supports provide better heat dissipation compared to the surrounding powder, the majority of heat is dissipated through the larger volume, solid structure. With the variation of heat dissipation through the support structure, the local microstructure can be influenced during both the solidification and the subsequent repeated heating and cooling process. It is difficult to understand the effect of the structural support on the local microstructure of the IN718 builds fabricated by L-PBF AM process.

## Experiments

The builds were fabricated with IN718 directly on the stainless-steel substrate. The preheat temperature in EOS M 290 machine is 80°C. Variable support heights were designed for five solid samples (20 x 20 x 20 mm). The support height varied from 5mm, 10mm, 15mm and 20mm of the solid sample height. These values are matched to the ratio of the support to the solid build: 1/4, 2/4, 3/4, 4/4.



Different support height: without support, 1/4, 2/4, 3/4, 4/4

Figure 1. Schematics of the as-built samples with different support thickness

The details of the laser parameters appear in Table 1. There were three sets of builds used in this study. Set B served as the baseline values for power, speed, and hatch distance while Set A and Set C varied the baseline parameters minus and plus 10%, respectively. Layer thickness remained constant for all parameter sets. There were 15 samples with different support thickness and three values of laser parameters. The as-build samples were evaluated using optical microscopy, scanning electron microscopy, and micro-hardness measurement.

**Table 1. Laser parameters for three sets**

	Set A (-10%)	Set B (Baseline value)	Set C (+10%)
<b>Power (W)</b>	256	285	313
<b>Speed (mm/s)</b>	864	960	1056
<b>Hatch distance (mm)</b>	0.09	0.11	0.12
<b>Layer thickness (mm)</b>	0.04	0.04	0.04

**Results**

The heat input and energy density were calculated using the following equation, with results shown in Table 2:

$$\text{Energy Density} = \frac{\text{Power (W)}}{\text{Speed (mm/s)} \times \text{Distance (mm)} \times \text{Layer Thickness (mm)}}$$

Set A with the lowest laser parameter values resulted in the highest heat input and energy density due to reduced laser-scan speed and hatch distance.

	Set A (-10%)	Set B (Baseline value)	Set C (+10%)
<b>Heat input (J/mm<sup>2</sup>)</b>	3.00	2.70	2.45
<b>Energy density (J/mm<sup>3</sup>)</b>	74.97	67.47	61.34

To characterize the microstructure, the solid samples were cut in two different orientations in this study. The representative microstructures are displayed in Figure 2(a) and 2(b) for XY and Z cutting direction, respectively. The hatch direction, including the 67° rotation between layers, and hatch distance can be clearly observed in

Figure 2(a). The representative microstructures from Z cutting directions are shown in 2(b).

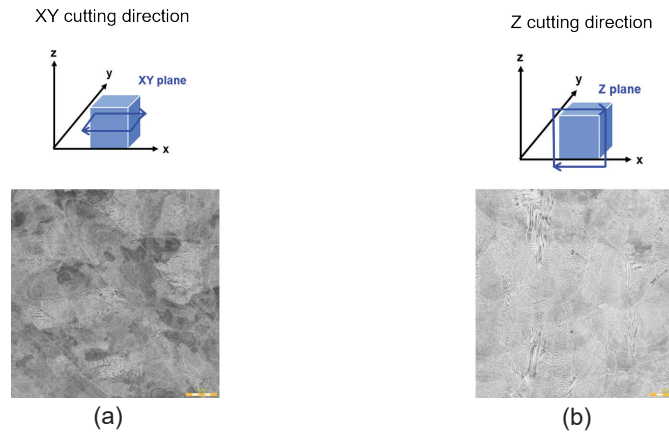


Figure 2. Optical images for XY cutting direction and Z cutting direction of the as-built samples

Figure 3 shows representative SEM images from all three build sets. Images (a) and (b) are from Set A, images (c) and (d) from Set B, and images (e) and (f) from Set C. For this study, only images from Z cutting directions were used. Layer thickness in these images ranges from 30-90 μm with an average value of 75 μm.

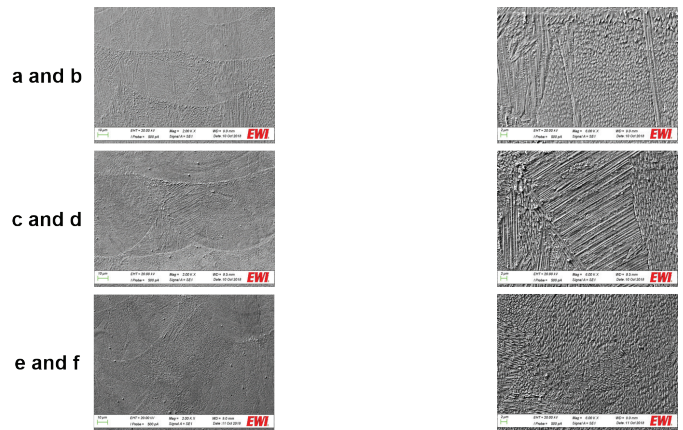


Figure 3. SEM images for XY cutting direction and Z cutting direction

EBSD technique was used to evaluate the microstructure texture of Set B and Set C (Figure 4). Grain growth and similar grain-size distribution was observed for both samples.

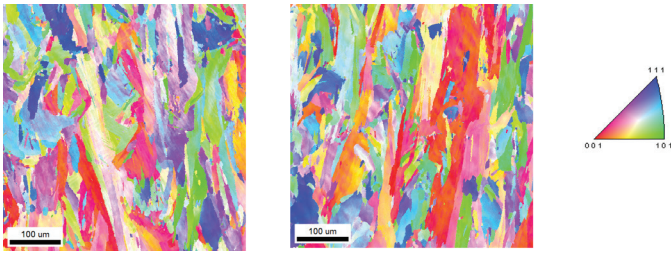


Figure 4. EBSD for the as-built samples

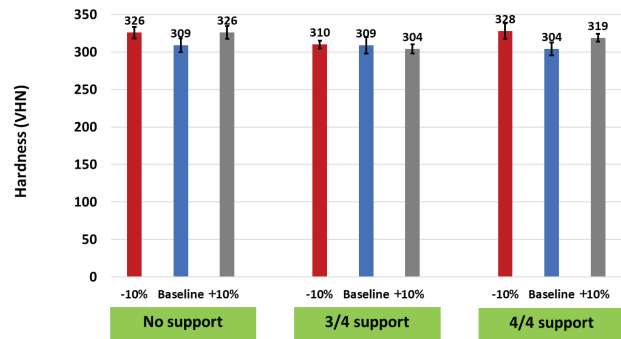


Figure 5. Averaged hardness values for no support, 3/4 and 4/4 support thickness

The Vickers hardness was measured for three conditions: no support, 3/4 support, and 4/4 support thickness (Figure 5). Average hardness values were similar for all three parameter conditions: -10%, baseline, and +10% for all three thickness conditions: no support, 3/4 support, and 4/4 support. Although a 5-8% increase in average hardness was observed in sample Set A (-10%) for no support and 4/4 support, these increased hardness values are within the error values.

## Conclusion

The as-built microstructure of Inconel 718 fabricated by L-PBF with variable support heights were characterized to (1) establish microstructural evolution depending

on the different heat dissipation conditions, and (2) comprehend the effect of the geometrical factor on the local microstructure. The support height with grid structure did not present a discernible difference in resulting microstructural evolutions. Moreover, differences in support thickness with grid structure did not result in significant variation in hardness. It is concluded that heat dissipation through grid structural support with different energy density values produces little effect on the local microstructure.

## References

1. W.E. Frazier, Metal Additive Manufacturing: A Review, J. Mater. Eng. Perform. 23 (2014) 1917-1928.
2. W.J. Sames, F.A. List, S. Pannala, R.R. Dehoff, S.S. Babu, The metallurgy and processing science of metal additive manufacturing, Int. Mater. Rev. 6608 (2016) 1-46.
3. J.H. Tan, W.L.E. Wong, K.W. Dalgarno, An overview of powder granulometry on feedstock and part performance in the selective laser melting process, Addit. Manuf. 18 (2017), 228-255.
4. H. Song, PhD. Thesis, "Multi-scale Microstructure Characterization for Improved Understanding of Microstructure-Property Relationship in Additive Manufacturing", 2016
5. G.A. Knorovsky, M.J. Cieslak, T.J. Headley, A.D. Romig, W.F. Hammett, INCONEL 718: A Solidification Diagram, Metall. Trans. A. 20 (1989) 2149-2158.
6. S.G.K. Manikandan, D. Sivakumar, M. Kamaraj, K. Prasad Rao, Laves Phase Control in Inconel 718 Weldments, Mater. Sci. Forum. 710 (2012) 614-619.
7. T.A. Krol, M.F. Zaeh, C. Seidel, Optimization of supports in metal-based additive manufacturing by means of finite element models, In: Proceedings of 23rd Annual International Solid Freeform Fabrication Symposium, August 6-8, 2011, Austin, United States, 2012, pp. 707-718.

**Hyeyun Song**, Project Engineer, is a member of EWI's additive manufacturing (AM) team and a post-doctoral research fellow at The Ohio State University. She has AM expertise in laser powder bed fusion, electron beam testing, selective laser sintering, and directed energy deposition. She has worked on projects in the metallurgy of advanced materials and microstructural analysis for conventional welding and AM processes and also has experience in nondestructive evaluation (NDE), ultrasonic and spot welding, and mechanical testing.